

The AMS Silicon Tracker: Performance Results from STS-91

J. Alcaraz³, B. Alpat⁵, G. Ambrosi², R. Battiston⁵, J. Berdugo³, B. Bertucci⁵, A. Biland⁷, S. Blasko⁵, M. Bourquin², W.J. Burger^{5*}, X.D Cai⁴, M. Capell⁴, J. Casaus³, M. Cristinziani², T.S. Dai⁴, P. Emonet², T. Eronen⁶, P. Extermann², E. Fiandrini⁵, A. Hasan⁷, T. Laitinen⁶, G. Lamanna⁵, A. Lebedev⁴, P. Levtchenko⁵, K. Lübelmeyer¹, W. Lustermann⁷, M. Menichelli⁵, M. Pauluzzi⁵, N. Produit², D. Rapin², F. Raupach¹, D. Ren⁷, M. Ribordy², E. Riihonen⁶, V. Shoutko⁴, H. Suter⁷, J. Torsti⁶, J. Vandenhirtz¹, D. Vité², W. Wallraff¹, M. Weisgerber¹, S.X. Wu⁴

¹*Physikalisches Institut, RWTH, D-52056 Aachen, Germany, supported by DLR, Cologne, Germany*

²*Université de Genève, CH-1211 Genève 4, Switzerland*

³*Unidad de Física de Partículas, CIEMAT, Avda. Complutense 22, E-28040 Madrid, Spain*

⁴*Massachusetts Institute of Technology, Cambridge, MA 02139, USA*

⁵*INFN-Sezione di Perugia and Università Degli Studi di Perugia, I-06100, Perugia, Italy*

⁶*Space Research Laboratory, Department of Physics, Turku University, FIN-20014, Finland*

⁷*Eidgenössische Technische Hochschule, ETH Zürich, CH-8093 Zürich, Switzerland*

* *corresponding author's mailing address: CERN-PPE, CH-1211 Genève 23*

Abstract

The Alpha Magnetic Spectrometer (AMS) is a detector designed to search for antimatter and dark matter in cosmic rays. AMS is programmed for installation on the International Space Station Alpha (ISSA) for an operational period of 3 years. The magnetic spectrometer uses 5.5 m² of silicon microstrip sensors to reconstruct charged particle trajectories. The AMS was flown on the NASA shuttle flight STS-91 in June 1998. In this contribution, we present results for the performance of the silicon tracker during the test flight.

1 Introduction

The AMS is designed to study the composition of cosmic rays with unprecedented sensitivity due to its large acceptance (0.5m²sr) and long observation time (3 years on the ISSA). The spectrometer is equipped with a silicon microstrip tracker providing 10 (30) μ m accuracy in the bending (non-bending) plane in the 1.5 kG field of the magnet, resulting in a momentum resolution of 7% in the range of 1-10 GeV/c/n. In order to verify the detector design, the AMS was flown on the NASA shuttle Discovery as part of the flight STS-91. All of the basic detector subsystems were present for the flight; the tracker was equipped with 38% of the total number of silicon sensors.

2 Shuttle Flight STS-91

The shuttle version of AMS consisted of 2.1 m² of double-sided silicon microstrip sensors (Batignani et al. 1989, Acciarri et al. 1994) arranged in six planes, four planes of plastic scintillator paddles, and an aerogel Cherenkov counter (n=1.035). The particle's mass is determined from the time-of-flight provided by the scintillators and the momentum of the silicon tracker. The energy loss measurements from the scintillators and the silicon tracker, together with the β of the time-of-flight, yield the charge of the particle. The sign of the charge is determined by the curvature of the reconstructed track. The Cherenkov detector provides electron-proton discrimination in the momentum range of 1-3.5 GeV/c. A layer of plastic scintillators located on the interior wall of the permanent magnet serve to veto stray trajectories and background produced by interactions in the material of the magnet. The AMS acceptance for the shuttle flight configuration was 0.31m²sr, corresponding to events with at least four tracker planes.

The shuttle flight STS-91 lasted 10 days, June 2-12, 1998. The shuttle Discovery operated at altitudes of 360 to 380 km above the surface of the earth, between the geographic latitudes $\pm 50^\circ$. The primary mission of the flight was the rendezvous with the Russian space station Mir. The periods dedicated to AMS operation

included 30 hours prior to the docking with Mir and 105 hours after separation from Mir, including 11 hours for an albedo measurement. Data collection continued throughout the flight aside from short interruptions during the docking and separation phases, and a three-hour pause during the second AMS observation period. The AMS data acquisition system livetime varied between 40 and 95% (for useful data), with recorded event rates of 700 to 100 Hz. A total of 99 million events were recorded.

3 Tracker Performance

The tracker performance can be characterized by the strip noise of the silicon sensors. The position measurement of the silicon microstrip detector uses the charge collected on the individual readout strips, thus one of the important limitations on the position resolution is detector noise. In addition, the relatively large size of the tracker (58,368 readout channels for the shuttle flight version) requires a good signal-to-noise ratio in order to maintain channel occupancy at an acceptably low level, without loss of detection efficiency.

The silicon tracker was powered three hours after the shuttle launch. Once the bias voltages of the silicon sensors had stabilized, no significant changes were observed in the dark current levels compared to the values measured during ground operation. The tracker calibration procedure determines the pedestals and the pedestal widths for each channel, and the average common noise widths. The ADC level of each channel is corrected by subtracting the common noise level, defined as the average ADC value recorded by the 64 channels of each preamplifier chip. The noise relevant for the tracker performance is the pedestal widths (σ_{ped}) after the common noise subtraction. The first calibration results from the flight indicated that the pedestals and pedestal widths of all readout channels were consistent with pre-launch values.

Tracker calibrations were made automatically every 30 minutes during data-taking. In addition, pedestals values were updated between calibrations using the event data. Abnormal interruptions of the data acquisition system also triggered a tracker calibration. A total of 738 calibrations were made during the flight with an average time between calibrations of 18 minutes.

The dominant influence on the tracker noise during the flight was the temperature. Figure 1 shows the average pedestal widths for the p-side strips (bending coordinate) of 50V and 100V silicon sensors, and the temperature recorded at the AMS magnet, versus the Mission Elapsed Time (MET). The tracker flown on the shuttle was composed of roughly equal numbers of 50V and 100V sensors. The tracker noise levels follow very closely the temperature evolution; the correlation is linear over the observed range of temperature with a slope of 0.025 ADC count/ $^{\circ}$ C. The silicon dark currents displayed an identical behavior.

The AMS temperature exhibits a nearly continuous decrease from the beginning of the flight to the second half of day 5 MET. The major influences on the AMS tempera-

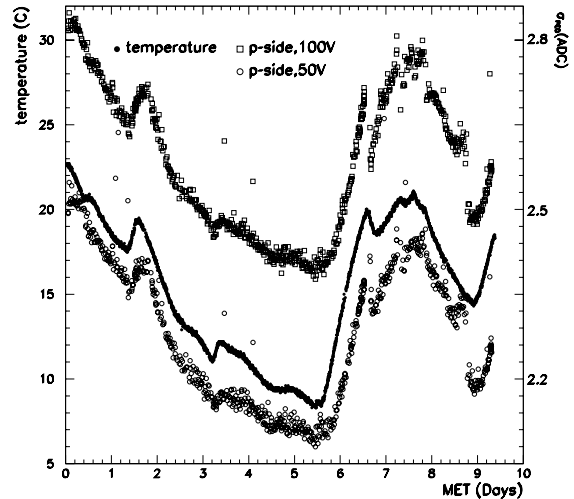


Figure 1: Comparison of AMS temperature and tracker noise during the STS-91 flight: temperature indicated on y-axis at left, p-side noise on y-axis at right.

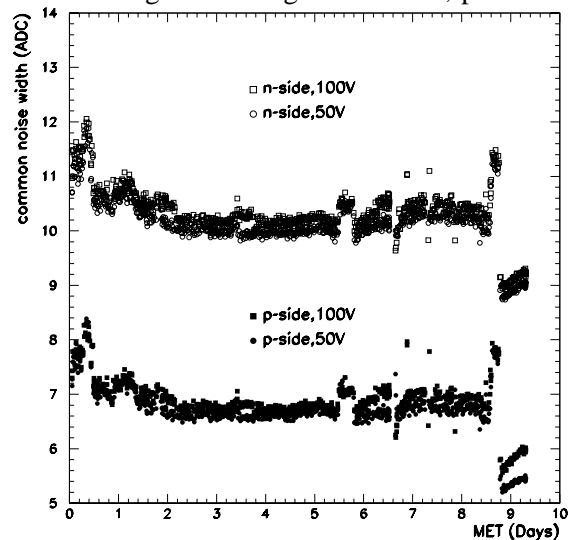


Figure 2: Tracker common noise levels during the STS-91 flight.

ture during this period were the opening of the payload doors, once the shuttle was installed in orbit, and the Mir docking, which placed the shuttle between Mir and the earth. After the separation with Mir, the AMS began its second observation period with the shuttle bay pointing towards deep space. At this time, the temperature at the detector began to rise. The constant increase was interrupted by powering down the detector for a period of three hours, after which data-taking resumed with the shuttle inclined at an angle of 20° with respect to the orbital zenith.

Figure 2 shows the average common noise widths for p and n-side strips. The observed changes in the common noise, abrupt shifts at well defined times, indicate that the tracker common noise was affected by activities on the shuttle. For example, the sudden jump and subsequent drop on day 5 MET correspond to a period when the Spacehab Universal Communication System (SHUCS) was operated. A SHUCS operation was also programmed for the middle of day 8 MET, along with several other activities involving other payload experiments, including deactivation of experiments which had been running throughout the flight. At this time, the tracker common noise increased by 10% before dropping to its lowest level. In general, the common noise changes observed during the flight did not affect the overall tracker noise performance, however the 20% decrease at the end of the flight was accompanied by a visible, though small (0.1 ADC count), decrease in the p-side pedestal widths (Fig 1).

The average noise level of the p-side strips can be compared to the measured cluster peak value for minimum ionizing particles (relativistic electrons and protons) of 25 ADC counts. The corresponding cluster signal-to-noise, defined by the total cluster charge divided by the root-mean-square of the pedestal widths of the member strips, varied with the temperature over the range of 7:1 to 8:1, consistent with the magnitude of the noise variation. The online signal threshold of $3.5\sigma_{ped}$ provided an acceptable rejection of p-side noise clusters.

The noise levels (σ_{ped}) of the n-side strips, which measure the coordinate in the non-bending plane, were 30% higher than for the p-side strips. The n-side strips of the silicon wafer collect the electrons liberated in the depleted region of the silicon. Due to the accumulation of negative surface charge on the n-side, the resolution is expected to be inherently worse. The difference observed with AMS sensors is larger however than expected. Inefficient charge collection across the readout gap is the problem. A redesign of the strip implantation on the n-side is planned to reduce the readout pitch, currently $208 \mu\text{m}$ (compared to $110 \mu\text{m}$ for the p-side readout strips).

The silicon tracker readout electronics were designed to maintain detector performance for incident particle charges of $Z \leq 10$. Figure 3 show the truncated sums of the energy loss measurements made in the silicon tracker for particles with $Z > 2$. The data correspond to 68 hours from the second AMS observation period with the detector pointing away from the earth. The curves in the figure represent Landau fits of the energy loss distributions of the indicated nuclei, identified by

comparing the energy loss in the tracker with the momentum measurement (selection made at the 1σ level based on the expected correlation between momentum and dE/dx). The results of this simple analysis show the possibilities offered by the silicon tracker for charge discrimination of light nuclei.

The linearity of the detector response with increasing charge is shown in Fig. 4, for average $\beta > 0.9$. The fitted line includes the charge values up to nitrogen; good linearity is obtained over this range. Several effects

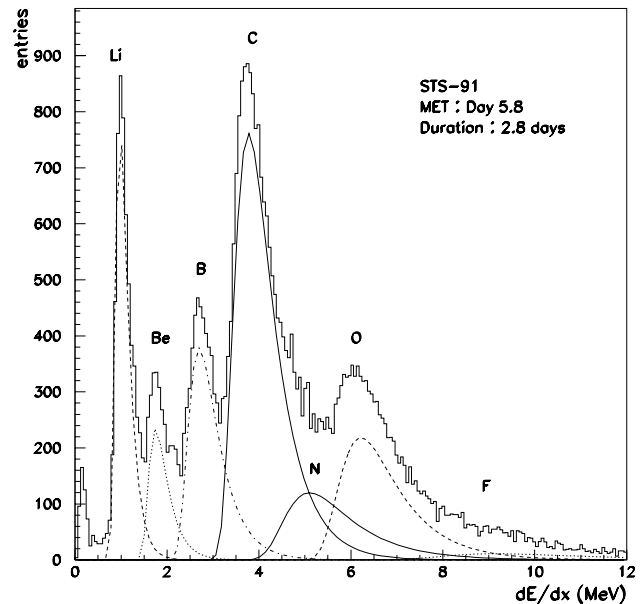


Figure 3: Truncated sums of the energy loss measurements of the silicon tracker for $Z > 2$ nuclei, the fits are described in the text.

may explain the non-linearity appearing at the highest Z . The dispersion of the pedestal widths observed at the preamplifier level required a rather high offset in the 12-bit ADC (1000 channels), reducing the effective dynamic range. Non-linear performance of the preamplifier or “saturation” effects in the charge collection in the silicon cannot be excluded.

The second important limitation on the tracker resolution is the alignment. The positions of the silicon sensors in the tracker planes were measured with a precision of 5-10 μm several months before the flight. The relative positions of the planes on their supporting structure were measured prior to installation in the magnet (50-100 μm precision). After the flight the detector alignment was checked using helium and carbon beams at GSI in D armstadt, Germany, and a proton beam at CERN in Gen eve, Switzerland. The alignment modifications determined from the test beam data did improve the track fits of the flight data. The tracker fit errors of the flight data, weighted with the expected measurement resolutions, are consistent with the expected momentum resolution. It is difficult to extract the position resolution directly from the flight data. Further insight on the contribution of possible misalignment to the detector resolution may be obtained by studying the behavior of quantities such as χ^2 distributions of fitted tracks, or eventually the mass resolution, which may reveal effects arising from the temperature variation observed during the flight. As seen earlier, such effects must be separated from other influences like increased detector noise.

We conclude with a figure which illustrates the general characteristics of the reconstructed momentum distribution of the flight data. Figure 5 show the reconstructed rigidity distribution for positive charge particles versus the shuttle position. The three-dimensional scatter plot displays the particle rigidity on the vertical axis, and the shuttle longitude (0° to 360°) and latitude (-60° to $+60^\circ$) on the x and y-axis. The particle distribution displays two main features: a rather constant width low rigidity band separated from a higher rigidity region whose minimum value increases as the detector approaches the equator, and a higher particle density in the regions closest to the magnetic poles. The two different rigidity regions can be identified with particles below and above the geomagnetic cutoff. The data of Fig. 5 correspond to one orbit of the shuttle (orbital period ~ 90 minutes).

4 Conclusion

The results of the AMS test flight are largely positive for the silicon tracker. No major problems were encountered. Electrically, the tracker performance was unaffected by the launch and operation in space, the effects observed are understood, e.g. n-side noise. Although there is no indication of a problem with the tracker mechanical design, the general question of temperature control is a concern. The principal objective of the flight was attained, a maximum amount of information from a working detector.

References

- Acciarri M., et al., 1994, Nucl. Instr. Meth., A351, 300.
 Batignani G., et al., 1989, Nucl. Instr. Meth., A277, 147.

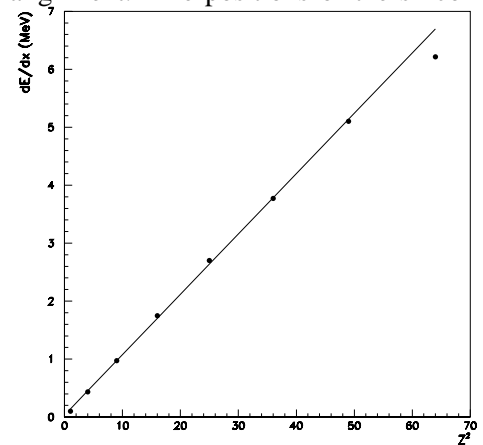


Figure 4: Silicon tracker energy loss peak values vs Z^2 .

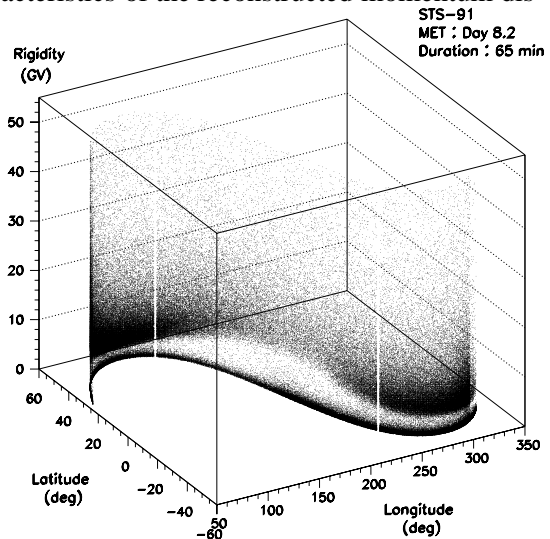


Figure 5: Reconstructed positive rigidity distribution versus shuttle position.